

Detailed Spectra of High-Power Broadband Microwave Emission from Intense Electron-Beam-Plasma Interactions

Keith G. Kato, Gregory Benford, and David Tzach

Department of Physics, University of California, Irvine, California 92717

(Received 10 January 1983)

For a relativistic electron beam penetrating an unmagnetized plasma, a change is seen in the emission spectrum from $\omega \sim \omega_p, 2\omega_p$ line emission to continuous $\omega \gg \omega_p$ emission, as $n_b/n_p \rightarrow 1$. High-power (of order megawatts per gigahertz) broadband radiation up to ~ 100 GHz suggests collective Compton-boosting mechanisms in a new regime of *superstrong* turbulence. Highly directional emission and magnetic field dependence agree with this interpretation.

PACS numbers: 52.40.Mj, 52.25.Ps

There is much recent interest in mechanisms whereby unstable electrostatic waves of a beam-plasma system convert into electromagnetic radiation. This basic problem applies to such diverse phenomena as auroral kilometric emission,^{1,2} type-III solar bursts,³⁻⁵ and plasma ω_p radiation in tokamaks.⁶

Two classes of theory dominate the discussion: weak turbulence (Thompson-type scattering of plasma waves of ion inhomogeneities to produce ω_p radiation^{7,8}) and strong turbulence (nonlinear electric-field terms driving, via the ponderomotive force, the formation of low-density solitons which emit ω_p and $2\omega_p$ radiation as they collapse⁴).

Both theory and experiment have concentrated on weakly perturbing beams ($n_b/n_p \ll 1$) which are at best mildly relativistic.^{9,10} Here we report detailed spectra from experiments with relativistic electrons ($\gamma \approx 3$) and $0.01 < n_b/n_p < 1$, with n_b (n_p) the beam (plasma) density. Because the emission is wholly unanticipated by either theory we call this the *superstrong* regime of beam-plasma turbulence.

In these experiments we fire an intense, annular, pulsed, relativistic electron beam along the axis of a plasma column and observe the radiation through radial side ports of the drift tube.¹¹ The electron accelerator is a standard Marx generator/pulse-forming transmission-line system. Typical operating values are $I = 128$ kA, $V = 893$ kV ($\gamma = 2.75$), 50 ns full width at half maximum, and 80 ns total pulse. The accelerator diode has an annular graphite cathode ($r \approx 3$ cm; $\Delta r \approx 1$ cm) with both foil and foilless operation. The drift-tube chamber is 20 cm diam \times 200 cm long, with suitable field coils to produce uniform axial magnetic fields B . The plasma source is a hydrated-Ti stack-washer gun, and plasma density is monitored by a 140-GHz microwave in-

terferometer. The spectrum is analyzed by a fifteen-channel spectrometer using two waveguide systems and two grating systems. This gives unequivocal determination of radiation frequency, simultaneous broadband frequency coverage from 5.85 to 40 GHz in 2.3-GHz bin widths, and absolute power measurements.¹² Values of n_b vary in the chamber because of thermal spreading. We give n_b at the anode; values in the region immediately near the microwave horns are lower by a factor of ~ 0.1 .

Figure 1 shows, for $B = 0$, a sample of our spectra as $f_p \equiv \omega_p/2\pi$ changes. Figure 1(a) has $f_p = 5.8$ GHz and shows a broadband plateau starting at about 20 GHz. The plateau shows little sign of rolloff as high as the sixth harmonic. Cylindrical modes have frequencies ≤ 1 GHz and cannot affect our results. Unfortunately, the f_p bin of the spectrometer was not active for these tests, and so we could not detect f_p emission. Figure 1(b) has $f_p = 24.7$ GHz, and the broadband plateau remains. Any ostensive f_p emission

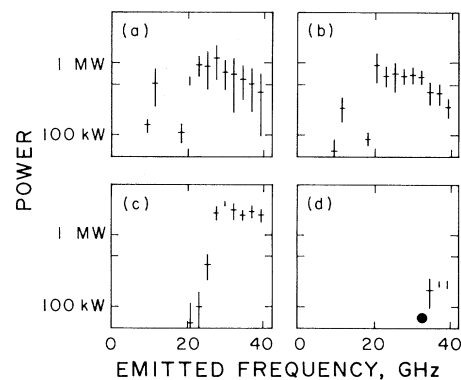


FIG. 1. Power spectrum for plasma frequency f_p of (a) 5.8 GHz; (b) 24.7 GHz; (c) 74.2 GHz; (d) 167 GHz. Power is given in 1/2.2 W/GHz. As f_p rises the broadband emission moves to higher frequencies.

would be within the broadband region, but no prominent feature appears above the broadband power level. Figure 1(c) has $f_p = 74.2$ GHz, and the broadband plateau is beginning to show some weak f_p dependence by moving upward in frequency and out of our observational window. Figure 1(d) has $f_p = 167$ GHz and little radiation.

The presence of radiation below f_p is not surprising, because the plasma has a spatial dependence $\sim \cos^2(\pi r/2R)$ and the beam can interact with plasma densities lower than the nominal value cited. Radiation far above $2f_p$ is unexpected, and we hypothesize the following mechanism.

A plasma wave (ω, \vec{k}) and beam electron ($\vec{p} = \gamma m \vec{v}$) collide at angle θ , and an EM wave (ω', \vec{k}') and beam electron ($\vec{p}' = \gamma' m \vec{v}'$) emerge at angle θ' . If we write the invariant four-momenta and use the approximation $|\vec{v}'| \approx |\vec{v}|$ and the electromagnetic dispersion relation $\omega'^2 = \omega_p^2 + \vec{k}'^2 c^2$, then¹³

$$\omega[1 - (kv/\omega)\cos\theta] = \omega'[1 - (k'v'/\omega')\cos\theta']. \quad (1)$$

If $\omega' \approx k'c \gg \omega_p$ and $\theta' \ll 1$, then

$$\omega' \approx \frac{2\gamma^2 \omega_p [1 - (kv'/\omega)\cos\theta]}{1 + \gamma^2 \theta'^2 + (\gamma\omega_p/\omega)^2}. \quad (2)$$

This yields a maximum possible frequency

$$\omega_{\max}' \approx 2\gamma^2 \omega_p (1 - \cos\theta). \quad (3)$$

Since for our experiments $\gamma = 2.75$, the frequency increase can be large if the angular factor is ~ 1 . The appearance of a γ^2 factor comes from the Compton effect ("Compton boosting").

Single-particle kinematics can thus explain high frequencies, but the high emitted power implies a collective process. Beam-plasma instability generates strong Langmuir turbulence⁴ and beam bunching.¹¹ We hypothesize a "collision" between bunched beam electrons and large-amplitude electrostatic waves generated by instability. We shall publish separately a two-step theory: bunching, followed by Compton boosting of electrostatic waves into electromagnetic emission. (This differs from a one-step electromagnetic instability, which can be suppressed by beam velocity spread.¹³) The required beam bunching, $\delta n_b/n_b \leq 0.1$, seems plausible.

The beam opening angle θ_b fixes a lower bound on the angle θ between electrons and plasma waves since we deal with beam-generated waves. The intrinsic angular spread of the waves, φ , will enter into θ roughly as $\theta \geq \theta_b + \varphi$. Thus a complex angular average will enter into any observed spectrum. This, plus the range of avail-

able outgoing angles θ' , means that emission must be broadband, not a set of lines.

This is distinctly different from earlier non-relativistic work,¹⁴ which observed some broadband electrostatic emission for $\omega \lesssim 3\omega_p$ at power levels $\sim 10^{-10}$ of ours.

In free-electron-laser language, we use an electrostatic wiggler, and beam bunching forces coherent emission. Our wiggler does not have a sharp k like free-electron lasers, because the unstable electrostatic spectrum has an unavoidable width. In free-electron lasers using magnetic wigglers,¹⁵ the highest available k is ~ 6 cm⁻¹, whereas ours is ~ 20 cm⁻¹. Mechanical wigglers have as strength parameter $\epsilon \equiv \Omega_w/kc \sim 1$, with Ω_w the cyclotron frequency of the wiggler's magnetic field. For our work, with use of beam electron trapping in the electrostatic waves to determine the wave strength, $\epsilon \sim 1$ as well, and use of free-electron-laser growth rates¹⁵ gives short amplification time of order nanoseconds. Thus there is an underlying analogy, though in our work the wiggler is spontaneously produced.

A convincing test of (3) would be a cutoff in the spectrum at $\omega \sim \gamma^2 \theta^2 \omega_p$. We used our grating in second- and third-order operation, ~ 120 GHz, and found significant power at frequencies up to the limit. While this indicates broad emission, for most values of ω_p the cutoff lies above 120 GHz. The 5.8-GHz case may be complicated by production of low-phase-velocity plasma waves, which (2) shows can yield very high frequencies. Future work in the ~ 200 -GHz range may provide information on the kinematic cutoff condition, (3).

Figure 2 shows, for $B = 0$ and $f_p = 18$ GHz, how the spectrum changes as n_b/n_p falls. Figure 2(a) has $n_b/n_p \leq 0.70$ and is the baseline spectrum. These experiments were performed with extremely careful control over f_p . Figure 2(a) shows a prominent rise in power of the bin near 20 GHz relative to its neighbors, and a pronounced roll-off in power in the higher frequencies of the broadband region. Figure 2(b) has $n_b/n_p \leq 0.17$, and shows prominent $f_p, 2f_p$ emission with $P(f_p)/P(2f_p) \approx 5$. Figure 2(c) has $n_b/n_p \leq 0.01$, and shows only a prominent f_p emission above a general power level in all other channels.

From these and other data we extract several salient features: (a) Total emitted power scales roughly as n_b^2 and is $\sim 10^6$ times that of a single-particle (incoherent) process. This was found as well in earlier experiments with the same setup.^{11,16} (b) Total power is not strongly dependent

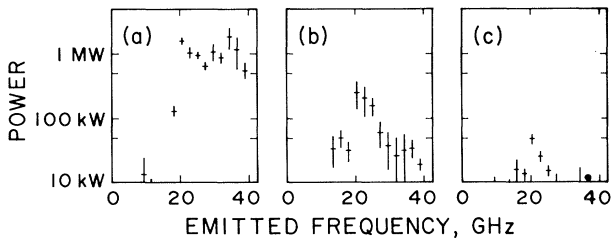


FIG. 2. Dependence of power on n_b with $f_p = 18$ GHz. (a) $n_b = n_0 = 10^{12}/\text{cm}^3$; (b) $n_b = n_0/4$; (c) $n_b = n_0/50$. As n_b falls, lines at $\sim f_p$ and $\sim 2f_p$ become more prominent.

on either beam energy or n_p . (c) The broadband radiation is highly directional, with maximum power received at a pickup angle corresponding to the opening half-angle (15°) of the beam (as measured by damage rods), and power lying within about a 60° range. We instrumented two ports of the drift tube with 26.5–40.0-GHz waveguide systems; one waveguide pickup pointed directly radially inward, as before, and the other (located farther down the drift tube to see approximately the same volume) at a fixed angle. We measured the ratio of power fluxes for these stations as a function of pickup angle.

We expect that electron momentum dominates the kinematics; hence the maximum. The $\sim 60^\circ$ range of radiation is consistent with the $1/\gamma$ half-angle expected from the radiation of relativistic particles.

Application of a weak magnetic field B_z demonstrates that f_p emission has a different mechanism from broadband emission. These experiments were performed with a Ti foil anode to ensure consistent diode behavior. As B_z increases from 0 to 800 G, the f_p line disappears while the broadband emission remains. Figure 3(a) shows, for $f_p = 18$ GHz and a Ti foil anode, the case $B = 0$; Fig. 3(b) shows the case $B = 800$ G where it is clear that the f_p line is gone. Figure 3(c) plots the power ratio of the f_p bin to the interpolated value of the f_p bin (using adjacent bins) as a function of B . The f_p line disappears at about 400 G, which is understandable as a change in the linear-wave dispersion relation. For a Langmuir wave traveling at angle θ with respect to an external magnetic field, the dispersion relation is

$$\omega^2 = \omega_p^2 \left(1 + \frac{3k^2}{\omega_p^2} \frac{k_B T_e}{m_e} + \frac{\omega_{ce}^2}{\omega_p^2} \sin^2 \theta \right). \quad (4)$$

For our experiment, $k \simeq \omega_p/v_b \simeq \omega_p/c$, $T_e \sim 5$ eV

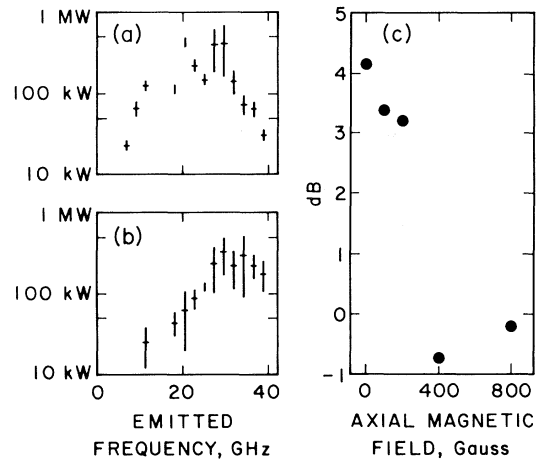


FIG. 3. Dependence of $\sim f_p$ line on axial field B_z . (a) $B_z = 0$, a prominent f_p line; (b) $B_z = 800$ G, f_p line gone. (c) Dependence of $f \sim f_p$ emission as B_z increases.

from Thompson scattering experiments on similar plasmas, and $\theta \simeq 15^\circ$ by both our damage-rod measurements and directivity measurements. The thermal and magnetic parts of the dispersion relation become equal at 135 G, and at 400 G the magnetic term is nine times the size of the thermal term. This apparently affects the line emission but not the Compton-boosted broadband radiation.

Further experiments and theory will be published later.

We thank Dr. Amnon Fisher and Dr. Scott Robertson for numerous helpful discussions, and Michael deLamare and William Main for their invaluable help. This work was sponsored by the Army Research Organization under Grant No. DAAG29-80-C-0013 and by the Air Force Office of Scientific Research under Grant No. 82-0233.

¹P. Palmadesso, T. P. Coffey, S. L. Ossakow, and K. Papadopoulos, *J. Geophys. Res.* **81**, 1762 (1976).

²J. E. Maggs, *J. Geomagn. Geoelectr.* **30**, 273 (1978).

³K. Papadopoulos, *Rev. Geophys. Space Phys.* **17**, 624 (1979).

⁴M. V. Goldman, G. F. Reiter, and D. R. Nicholson, *Phys. Fluids* **23**, 388 (1980).

⁵H. P. Freund and K. Papadopoulos, *Phys. Fluids* **23**, 732 (1980).

⁶I. H. Hutchinson, K. Molvig, and S. Y. Yuen, *Phys. Rev. Lett.* **40**, 1091 (1978).

⁷D. F. Smith, *Adv. Astron. Astrophys.* **7**, 147 (1970).

- ⁸D. B. Melrose, *Space Sci. Rev.* 26, 3 (1980).
- ⁹D. A. Whelan and R. L. Stenzel, *Phys. Rev. Lett.* 47, 95 (1981).
- ¹⁰P. Y. Cheung, A. Y. Wong, C. B. Darrow, and S. J. Qian, *Phys. Rev. Lett.* 48, 1348 (1982).
- ¹¹G. Benford, D. Tzach, K. Kato, and D. F. Smith, *Phys. Rev. Lett.* 45, 1182 (1980).
- ¹²Keith G. Kato, Ph.D. dissertation, University of California, Irvine, 1983 (unpublished), and to be published.
- ¹³S. A. Kaplan and V. N. Tsytovich, *Plasma Astrophysics* (Pergamon, New York, 1973).
- ¹⁴J. Greenly, A. Cavalli, and J. E. Walsh, *Phys. Fluids* 20, 1762 (1977).
- ¹⁵G. Bekefi and R. E. Shefer, *J. Appl. Phys.* 50, 5158 (1979); G. Bekefi, *J. Appl. Phys.* 51, 3081 (1980).
- ¹⁶D. Tzach, G. Benford, C. W. Roberson, and N. Rosstoker, *J. Appl. Phys.* 50, 6241 (1979).